Thin Solid Films 518 (2010) 5546–5552

Contents lists available at ScienceDirect

Thin Solid Films

journal homepage: www.elsevier.com/locate/tsf

Influence of carbon chemical bonding on the tribological behavior of sputtered nanocomposite TiBC/a-C coatings

M.D. Abad [a], J.C. Sánchez-López [a,*], M. Brizuela [b], A. García-Luis [b], D.V. Shtansky [c]

[a] Instituto de Ciencia de Materiales de Sevilla (CSIC-Univ. Sevilla), Avda. Américo Vespucio 49, 41092-Sevilla, Spain
[b] Fundación Inasmet-Tecnalia, Mikeletegui Pasealekua 2, 20009 Donostia-San Sebastián, Spain
[c] State Tecnological University "Moscow Institute of Steel and Alloys", Leninsky pr. 4, 119049-Moscow, Russia

A R T I C L E   I N F O

Article history:
Received 16 July 2009
Received in revised form 21 January 2010
Accepted 15 April 2010
Available online 25 April 2010

Keywords:
Titanium boron carbide
Nanocomposites
Amorphous carbon
X-ray photoelectron spectroscopy
Raman
Wear
Friction
Hardness

A B S T R A C T

The tribological performance of nanocomposite coatings containing Ti–B–C phases and amorphous carbon (a-C) are studied. The coatings are deposited by a sputtering process from a sintered TiB_2:TiC target and graphite, using pulsed direct current and radio frequency sources. By varying the sputtering power ratio, the amorphous carbon content of the coatings can be tuned, as observed by X-ray photoelectron spectroscopy (XPS) and Raman spectroscopy. The crystalline component consists of very disordered crystals with a mixture of TiB_2/TiC or TiB_xC_y phases. A slight increase in crystalline order is detected with the incorporation of carbon in the coatings that is attributed to the formation of a ternary TiB_xC_y phase. An estimation of the carbon present in the form of carbide (TiB_xC_y or TiC) and amorphous (a-C) is performed using fitting analysis of the C 1s XPS peak. The film hardness (22 to 31 GPa) correlates with the fraction of the TiB_xC_y phase that exists in the coatings. The tribological properties were measured by a pin-on-disk tribometer in ambient conditions, using 6 mm tungsten carbide balls at 1 N. The friction coefficients and the wear rates show similar behavior, exhibiting an optimum when the fraction of C atoms in the amorphous phase is near 50%. This composition enables significant improvement of the friction coefficients and wear rates ($\mu\sim0.1$; $k<1\times10^{-6}$ mm^3/Nm), while maintaining a good value of hardness (24.6 GPa). Establishing the correlation between the lubricant properties and the fraction of a-C is very useful for purposes of tailoring the protective character of these nanocomposite coatings to engineering applications.

1. Introduction

During the past decade, many research efforts have focused on the development of multicomponent and multifunctional coatings based on a nanocomposite design, with the purpose of increasing a material's performance under severe corrosion, oxidation, and environmental conditions [1–3]. Nanocomposite coatings are typically formed from the combination of at least two immiscible phases: two nanocrystalline phases or, more commonly, an amorphous phase surrounding nanocrystallites of a secondary phase, typically consisting of nitrides, carbides, borides, or silicides. Ti–B–C coating systems are one of the promising nanocomposite coatings systems exhibiting superior hardness, good tribological properties, and high oxidation and corrosion resistance [4–9]. Many variations of Ti–B–C nanocomposites have been produced, due to the feasibility of plasma-assisted physical vapour deposition [4–23] and chemical vapour deposition methods [24,25] that allow the formation of metastable phases out of thermodynamic equilibrium. The chemical composition and desired properties of the coatings can thus be tuned depending on the deposition technique and the experimental conditions used. Fig. 1 shows a ternary diagram that summarizes the selection of Ti–B–C coatings found in a literature survey. For instance, in the early works of Mitterer et al. [4] Ti–B–C coatings were produced by sputtering of a target of TiB_2 in an argon and C_3H_8 atmosphere. He was the first to suggest that the formation of a ternary TiB_xC_y phase derived from the incorporation of C or B into the TiB_2 or TiC phase, respectively. Almost simultaneously, Knotek et al. [5] sputtered a TiB_2 target with an Ar/CH_4 atmosphere, and discussed the possible incorporation sites of carbon in the hexagonal TiB_2 cell. The new phase observed in this work showed exceptionally good values of hardness (~70 GPa). Years later, Mitterer et al. [9] deposited Ti–B–C coatings by the direct co-sputtering of TiB_2 and TiC targets with Ar. The elemental composition was found to follow to the quasi-binary TiB_2–TiC tie line of the Ti–B–C phase diagram (cf. Fig. 1). The hardness values of the coatings were extremely high, reaching values of ~70 GPa for 20–25 at.% C. This represents an improvement with respect to the individual phases (68 GPa for TiB_2 and 42 GPa for TiC). Mitterer attributed this superhardness to a nanocomposite structure comprising nanocrystals of TiC in a quasi-amorphous TiB_2 phase, or a nanocrystalline TiB_2 dispersed in a quasi-amorphous TiC phase. In conclusion, Ti–B–C

---

[*] Corresponding author.
E-mail address: jcslopez@icmse.csic.es (J.C. Sánchez-López).

0040-6090/$ – see front matter © 2010 Elsevier B.V. All rights reserved.
doi:10.1016/j.tsf.2010.04.038

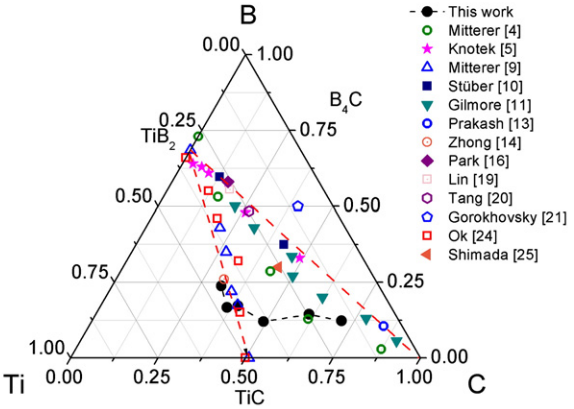

Fig. 1. Elemental chemical composition of the deposited TiBC/a-C nanocomposite coatings on a Ti–B–C ternary diagram. The lines show some of the binary systems formed between TiB$_2$, TiC and C. A selection of Ti–B–C coatings found in a literature survey is also included.

coatings exhibiting high hardness with a strong dependence on the deposition process were demonstrated by many authors, although the origins of the composition and mechanical property relationship were not thoroughly assessed (nanocomposite or ternary TiB$_x$C$_y$ phase).

Many authors have synthesized Ti–B–C coatings searching for a hardness improvement, but the tribological properties were not the primary object of study. Gilmore et al. [11] was the first to deposit Ti–B–C films by sputtering TiB$_2$ and C targets, resulting in nanocomposite coatings with self-lubricating properties. The carbon phase dispersed in a hard wear-resistant matrix can act as a reservoir of the lubricant phase throughout the thickness of the hard coating. Studies using X-ray photoelectron spectroscopy (XPS) of the C 1s confirmed the existence of the TiB$_x$C$_y$ phase, previously revealed by X-ray diffraction (XRD) for Mitterer [4] and Knotek [5], and the segregation of carbon in the form of an amorphous matrix (a-C; labeled as DLC by the authors). The carbon was preferentially incorporated in the TiB$_2$ lattice, and it was necessary to attain an overall C content of approximately 50 at.% before the lattice became saturated. Friction reduction was achieved due to the formation of a distinct carbonaceous phase. It was found that a minimum of approximately 20 at.% of a-C phase was required to provide a significant lubricating effect, although the hardness was reduced.

The purpose of this paper is to report the correlation of structure, mechanical properties and tribological performance of magnetron sputtered TiBC/a-C thin films. In the present study, we have used an alternative approach to synthesize multiphase hard coatings with a low friction coefficient by co-sputtering a unique TiC:TiB$_2$ (60:40) combined target and a lubricant phase such as graphitic carbon. Afterwards, the mechanical and tribological properties are evaluated on the relative amount of amorphous and crystalline phases. The samples are labeled for simplicity as TiBC/a-C, although a mixture of different crystalline phases and variable stoichiometry may be present.

2. Experimental details

Ceramic targets of TiC:TiB$_2$ were produced in a ratio 60:40 using the self-propagating high-temperature synthesis method (SHS), described in detail in reference [15]. The elemental composition was found to be 42.4 at.% Ti, 30.8 at.% B and 26.8 at.% C, with a residual porosity around 7.5%. The Ti–B–C coatings were prepared by Ar$^+$ sputtering of the combined TiC:TiB$_2$ and graphite targets. The magnetrons were connected to radio frequency (graphite target, Goodfellow, 99.5%) and pulsed direct current (d.c.) sources (TiC:TiB$_2$ target), at frequencies of 13.56 MHz and 50 kHz, respectively. The pressure of the vacuum chamber was measured before deposition as 3×10^{-4} Pa, increasing to 0.60 Pa during film growth. A series of TiBC/a-C coatings was prepared by changing the sputtering power ratio (R), which is defined as the ratio of sputtering power applied to the graphite target in respect to the TiC:TiB$_2$ target ($R = P_C/P_{TiC:TiB_2}$), from 0 to 3. The typical power values applied to the TiC:TiB$_2$ target span between 125 and 250 W, while those applied to the graphite target were varied from 0 to 375 W. Film deposition always began by first sputtering the mixed TiC:TiB$_2$ target at 250 W (underlayer). Second, the magnetron with the graphite target was switched on and the selected values of sputtering power for each target were fixed for TiBC/a-C coating deposition, as summarized in Table 1. The magnetron heads are tilted by 45 °C with respect to the vertical axis and placed in a sputtering-down configuration. The substrates were mounted on a rotary sample-holder, situated at 10 cm from the targets. Prior to starting the deposition, an Ar$^+$ etching of the substrates was performed at 7 Pa and 1000 V (d.c.) for 1 h to remove any adventitious contamination layer. A rotation speed of 10 rpm was used to ensure homogeneity. The temperature was found to vary in the within the range of 150 and 200 °C under exposure to plasma. No additional heating of the substrate was applied. A negative d.c. bias of 100 V was applied to the samples during the whole deposition process. The growth time was approximately 5 h and the film thickness ranged from 1.0 to 1.5 µm. The substrates used were silicon, NaCl and tempered M2 steel disks (hardness = 16 GPa). The steel substrates were polished ($Ra < 0.01$ µm) and cleaned ultrasonically with acetone and ethanol.

The crystal structure of the films was examined by XRD using an incidence angle of 1° and Cu K$_\alpha$ radiation in a Siemens D5000 diffractometer. A Philips CM200 microscope operating at 200 kV and equipped with a parallel detection electron energy-loss spectroscopy (EELS) spectrometer from Gatan (766–2 k) was used for the evaluation of the film microstructure and chemical composition. Raman spectra measurements (200–2000 cm^{-1}) were carried out with a LabRAM Horiba Jobin Yvon spectrometer equipped with a charge-coupled device detector and a He–Ne laser (532 nm) at 5 mW. All the samples were analyzed with 100 s exposure times and confocal holes of 100 µm. XPS measurements were carried out using a Leybold–Heraeus spectrometer equipped with an EA-200 hemispherical electron multichannel analyzer, operating with a non-monochromated Mg K$_\alpha$ X-ray source (1253.6 eV). A five-minute Ar$^+$ sputtering at a voltage of 3 kV and a pressure of 2×10^{-6} Pa was carried out in order to remove the surface contamination. Fitting analysis was performed on the C 1s peak in order to estimate the relative amount of the different carbon bonds present (carbides and amorphous carbon). Data fitting was carried out by a least squares routine supplied by XPS Peak Fitting Programme 4.1 [26], using mixed Gaussian–Lorentzian peaks.

The mechanical properties were measured on coated M2 steel disks with a Fischercope H100 dynamic microprobe instrument using a conventional Vickers indenter, at loads up to 10 mN. The maximum load was selected in such a way that the maximum indentation depth did not exceed 10–15% of the coating thickness, thus avoiding

Table 1
Synthesis conditions and elemental composition of the TiBC/a-C coatings.

Coating	Synthesis conditions		Elemental composition			
	P_C W	$P_{TiC:TiB_2}$ W	C %	B %	Ti %	Film stoichiometry
R0	–	250	31	24	45	$TiB_{0.53}C_{0.70}$
R0.2	50	250	36	17	47	$TiB_{0.36}C_{0.78}$
R0.5	125	250	40	17	43	$TiB_{0.39}C_{0.90}$
R1	250	250	49	12	39	$TiB_{0.31}C_{1.27}$
R2	250	125	61	14	25	$TiB_{0.59}C_{2.48}$
R3	375	125	71	12	17	$TiB_{0.75}C_{4.35}$